Histogram Analysis Parameters ADC for Distinguishing Ventricular Neoplasms of Ependymoma, Choroid Plexus Papilloma, and Central Neurocytoma

Authors' Contribution:
Study Design A
Data Collection B
Statistical Analysis C
Data Interpretation D
Manuscript Preparation E
Literature Search F
Funds Collection G

ABCDEF 1 **Chen Chen**
G 1 **Cui-ping Ren**
F 1 **Rui-chen Zhao**
B 2 **Jiang-wei Ding**
G 1 **Jing-liang Cheng**

1 Department of Magnetic Resonance Imaging (MRI), First Affiliated Hospital of Zhengzhou University, Zhengzhou, Henan, P.R. China
2 Department of Neurosurgery, First Affiliated Hospital of Zhengzhou University, Zhengzhou, Henan, P.R. China

Corresponding Author: Cui-Ping Ren, e-mail: rcp810@sohu.com
Source of support: National key R&D Program of China (2016YFC0106900)

Background: To determine if histograms of ADC can be used to differentiate ventricular ependymomas, choroid plexus papillomas (CPPs), and central neurocytomas (CNCs).

Material/Methods: We retrospectively reviewed records from 185 patients from 1 January 2014 to 1 November 2018. We finally included a total of 60 patients: 36 (60.00%) had histologically confirmed ependymomas, 10 (16.67%) had CPPs, and 14 (23.33%) had CNCs, as determined by routine MRI scanning at 3.0T. The ADC histogram features were derived and then compared by Kruskal-Wallis test (they were not normally distributed). Bonferroni test was used to compare the 2 groups and then we determined the ROC.

Results: Ependymomas had significantly higher mean, perc.01%, perc.10%, perc.50%, perc.90%, and perc.99% than CNCs. Ependymomas had significantly lower skewness than CNCs. Histogram metrics derived from mean, perc.01%, perc.10%, perc.50%, and perc.90% were significantly lower in the CNCs group than in the CPPs group. CPPs showed significantly lower skewness than CNCs. A threshold value of 86.50 for perc.50% to predict ependymomas from CNCs was estimated (AUC=0.97, sensitivity=97.20%, specificity=85.70%). Optimal diagnostic performance to predict CPPs from CNCs (AUC=0.96, sensitivity=100.00%, specificity=85.70%) was obtained when setting Perc.50%=84.00 as the threshold value.

Conclusions: The ADC histogram analysis may help to discriminate ependymomas, CPPs, and CNCs.

MeSH Keywords: **Brain Neoplasms • Cerebral Ventricle Neoplasms • Diffusion Magnetic Resonance Imaging**

Full-text PDF: https://www.medscimonit.com/abstract/index/idArt/915398

📄 1410   📊 4   📈 3   📖 15

Background

Histopathologic examination is still the criterion standard for diagnosis of brain tumors. Surgical biopsies entail potential morbidity and mortality risks. The intraoperative microscopic diagnosis error rate is 3% to 8% [1]. Accurate diagnosis in neuroimaging before treatment is usually necessary.

Ependymomas, choroid plexus papillomas (CPPs), and central neurocytomas (CNCs) are sometimes difficult to distinguish. Ependymomas and CPPs are usually seen in children and adults, while CNCs are more common in adults. They all can show as lobulated masses. Typical CPPs show homogeneous signal intensity, while CNCs have heterogeneity in T1WI and T2WI, and on DWI the solitary tissues of the tumors usually display reduced diffusion because of high tumor cellularity. Susceptibility artifacts can be seen in ependymomas because of internal calcifications or hemorrhage (calcifications in 50% of lesions, hemorrhage in approximately 10%) [2]. CPPs can show flow voids. CNCs usually contain cystic regions, calcifications, and tumor vessels, which appear as signal voids on MRI [3]. CNCs had a "bubbly" appearance on T2WI due to clusters of cysts of varying sizes [4]. Due to the plasticity of ependymomas, they can grow through the foramina of Luschka, Magendie, and magnum [5]. CPPs in the lateral ventricles may enter into the foramina of Monro, and the tumors in the fourth ventricle can go through the foramina of Luschka [6]. CPPs exhibit elevated choline peak and depressed NAA. Elevated myoinositol levels on MRS suggest the presence of CPPs [7]. CNCs show increased choline: creatine ratio, and glycine (3.55 ppm) on MRS is a rather specific marker [8]. CPPs and CNCs can result in dilation of ventricles to varying degrees.

The aim of this study was to use ADC histograms of solid components to discriminate among ependymomas, CPPs, and CNCs.

Material and Methods

Patients

We used the surgical pathology database for the period of January 1, 2014 to November 1, 2018 in our hospital. Exclusion criteria were: (1) patients who received treatment before surgery; (2) not confirmed histologically by biopsy; (3) inadequate image quality; and (4) without enhanced-T1WI. A total of 60 patients (36 ependymomas, 10 CPPs, and 14 CNCs) met the inclusion criteria for our study. All methods were performed in accordance with the relevant guidelines and regulations, and all informed consent requirements were met. This retrospective study was approved by the Institutional Ethics Review Committee of our hospital.

Image analysis

Patients were examined with a 3T MR scanner (Siemens Skyra) with standard head coil. The MRI scan protocols included: axial T1WI (TR/TE=260.0/2.46 ms), axial T2WI (TR/TE=3800/93.0 ms), axial FLAIR (TR/TE=4500/93.0 ms), sagittal T2WI (TR/TE=4200/79 ms), axial DWI (b=0 and 1000 s/mm^2, TR/TE=3500/119 ms, field of view=230 mm, thickness=5 mm, intersection gap =0.3mm, and layers=20), and contrast-enhanced T1WI (flow rate=2.0 mL/s, dose=0.2 ml/kg).

The ROI on the ADC image of the largest lay was selected by reference to enhanced-T1WI, DWI, and T2WI. One physician delineated ROI manually along the edge of the lesion and filled it in with red, excluding the various necrotic and cystic regions. MaZda software (version 4.7, the Technical University of Lodz, Institute of Electronics, *http://www.eletel.p.lodz.pl/mazda/*) was used to calculate ROI and get histogram parameters, including mean value, variance, skewness, kurtosis, and percentile values.

Statistical analysis

Non-normally distributed data were assessed using the Kruskal-Wallis test. Multiple testing used Bonferroni correction. Non-normally distributed are shown as medians. Sensitivity, specificity, and area under the curve were calculated for the diagnostic procedures. Thresholds were chosen to maximize the Youden index. All statistical analyses were performed using SPSS (SPSS 23.0). A P-value <0.05 was considered to be statistically significant.

Results

From January 2015 until November 2018, a total of 60 patients were finally selected for the study. There were 36 patients with ependymomas, 10 patients with CPPs, and 14 patients with CNCs (Figure 1). More details about tumor characteristics are provided in Table 1 and Figure 2. Because all measurements were non-normally distributed, data are presented as medians.

There was a significant difference in average age of patients among the different tumor types. There was a significant difference in ADC percentile values (p=0.000), mean (p=0.000), variance (p=0.008), and skewness (p=0.020) (Table 2). We found no significant difference in kurtosis. The Bonferroni test was used to compare the 2 groups, and we found that mean, skewness, and ADC percentile values between ependymomas and CNCs were significantly different (p<0.017). Mean, skewness, perc.01%, perc.10%, perc.50%, and perc.90% between CPPs and CNCs were significantly different (p<0.017). Differences between ependymomas and CPPs were not statistically significant (p>0.017). Ependymomas showed significantly higher mean,
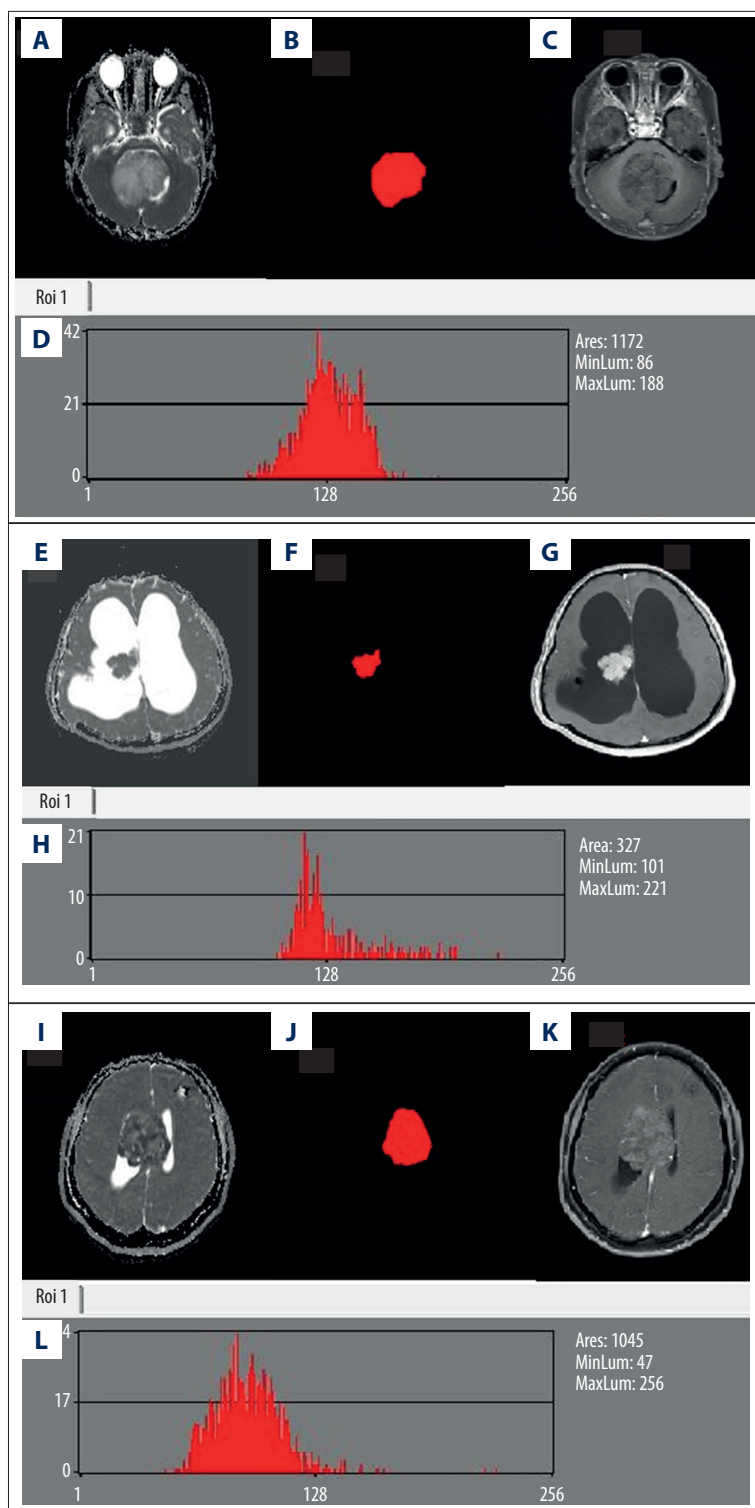
Figure 1. Representative cases of ependymomas (A–D), CPPs (E–H), and CNCs (I–L). The left column showed axial ADC of a 3-year-old boy patient with ependymoma, that of a 29-year-old woman with CPP, and that of a 28-year-old woman with CNC (A, E, I). Enhanced-T1WI were conducted (C, G, K). Corresponding ROI and histogram maps are shown (B, D, F, H, J, L).

perc.01%, perc.10%, perc.50%, perc.90%, and perc.99% than CNCs. Ependymomas had significantly lower skewness than CNCs. Histogram metrics derived from mean, perc.01%, perc.10%, perc.50%, and perc.90% were significantly lower in CNCs than in CPPs. CPPs showed significantly lower skewness than CNCs.

AUCs for the most significant ADC histogram parameters are shown in Table 3 and Figure 3. The perc.50% had better discriminative powers to differentiate ependymomas and CNCs, with optimal cutoff values as 86.50, yielding a sensitivity of 97.20% and a specificity of 85.70% (Table 3). Optimal diagnostic

Table 1. Characteristics of patients with ependymomas, CPPs, and CNCs.

	Ependymomas	CPPs	CNCs
Number	36	10	14
Age, years	7 (1–66)	16 (1–51)	26.5 (18–38)
Sex			
Male	18	4	11
Female	18	6	3

performance to predict CPPs from CNCs (AUC=0.96, sensitivity=100.00%, specificity=85.70%) was obtained when setting perc.50%= 84.00 as the threshold value (Table 4).

Discussion

The purpose of the study was to analyze the histograms of ADC maps for differentiating ependymomas, CPPs, and CNCs.

Previous studies have used histograms of ADC in the differentiation of fourth ventricular tumors and posterior fossa tumors [9–11]. Histograms can show more descriptive information about ADC values than mean ADC. The results show that ADC histogram parameters, especially perc.50%, might help to differentiate them.

Skewness and kurtosis

Skewness is a parameter that measures a histogram's asymmetry. In theory, positive skewness means that the main distribution of the mass is focused on the left-hand side of the graph, which indicates that there is high cellularity or possibility of malignancy. Negative skewness, where the main distribution of the mass is focused on the right-hand side of the graph, suggests a large amount of cystic or edematous tissue [12]. When ROIs were placed, various necrotic and cystic areas were excluded. Therefore, skewness was mainly manifested as positive. CNCs showed the highest skewness, followed by ependymomas and CPPs. Although the sensitivities were not high, the results were consistent with the variation trend of skewness,
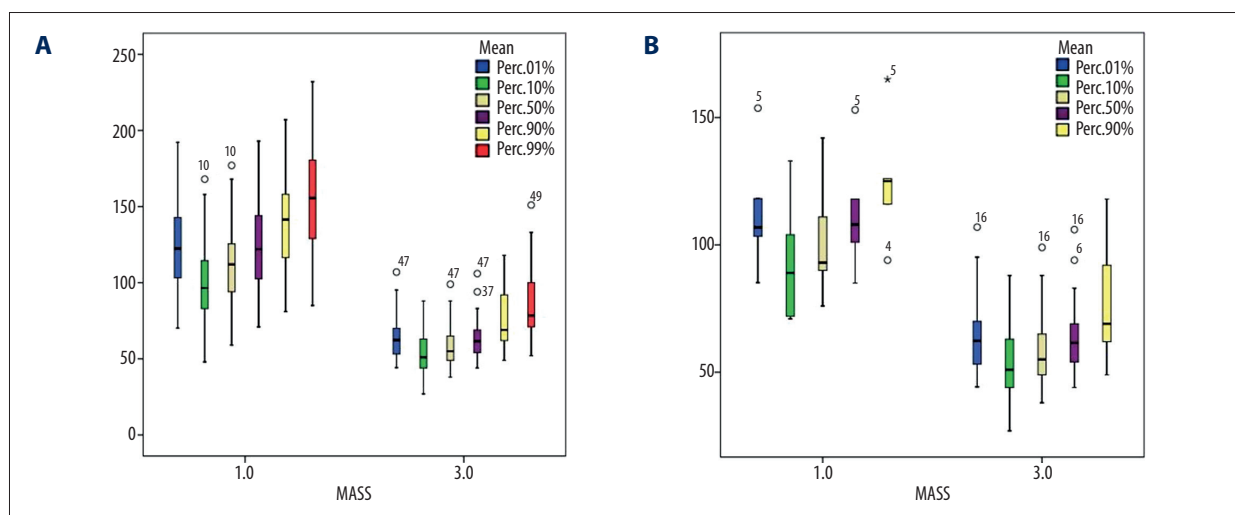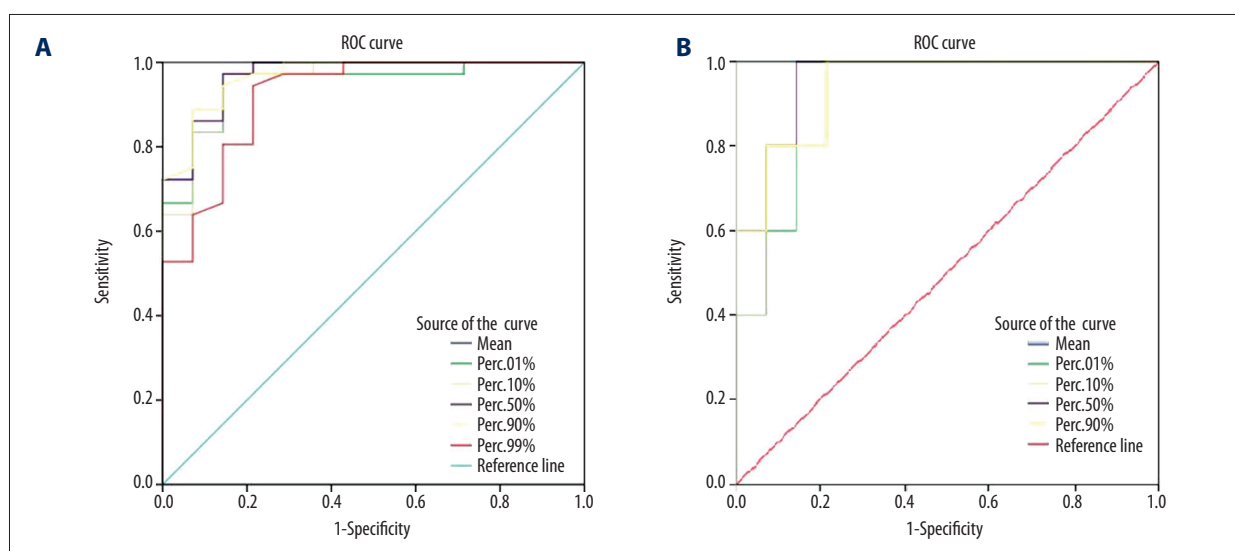

Figure 2. The left picture shows mean, perc.01%, perc.10%, perc.50%, perc.90%, and perc.99% for the patient groups with ependymomas and CNCs. The right picture shows mean, perc.01%, perc.10%, perc.50%, and perc.90% for patient groups with CPPs and CNCs.

Table 2. Parameters of patients with ependymomas, CPPs, and CNCs.

Tumor	Skewness	Kurtosis	Mean	Variance	Perc.01%	Perc.10%	Perc.50%	Perc.90%	Perc.99%
Ependymomas	0.22	−0.07	122.36	94.03	96.50	112.00	112.00	141.50	155.50
CPPs	0.035	−0.15	106.89	66.93	89.00	93.00	108.00	125.00	133.00
CNCs	0.58	0.80	62.35	42.77	51.00	55.00	61.50	69.00	78.50
H	7.804	5.480	27.132	9.564	25.152	26.035	27.578	27.324	22.129
p	0.020	0.065	0.000	0.008	0.000	0.000	0.000	0.000	0.000

Table 3. ROC analysis of ADC histogram features for discriminating ependymomas from CNCs.

Parameters	AUC	Cutoff value	Sensitivity	Specificity	p
Mean	0.966	70.07	100.00	78.60	0.000
Skewness	0.710	0.53	57.10	77.80	0.002
Perc.01%	0.948	69.50	97.20	85.70	0.000
Perc.10%	0.956	76.00	97.20	85.70	0.000
Perc.50%	0.968	86.50	97.20	85.70	0.000
Perc.90%	0.968	95.50	94.40	85.70	0.000
Perc.99%	0.921	101.00	94.40	78.60	0.000

Figure 3. ROC curves of significant ADC histogram features for differentiating among ependymomas, CPPs, and CNCs. The left picture shows ROC curves of mean, perc.01%, perc.10%, perc.50%, perc.90%, and perc.99% for differentiating ependymomas and CNCs. The right picture shows ROC curves of mean, perc.01%, perc.10%, perc.50%, and perc.90% for differentiating CPPs and CNCs.

Table 4. ROC analysis of ADC histogram features for discriminating CPPs from CNCs.

Parameters	AUC	Cutoff value	Sensitivity	Specificity	p
Mean	0.943	84.49	100.00	85.70	0.004
Skewness	0.886	0.34	64.30	100.00	0.012
Perc.01%	0.943	68.00	100.00	85.70	0.004
Perc.10%	0.943	73.50	100.00	85.70	0.004
Perc.50%	0.957	84.00	100.00	85.70	0.003
Perc.90%	0.943	93.00	100.00	78.60	0.004

suggesting that there was a potential difference in the density of the 3 types of tumor cells. The kurtosis of histograms was the statistic describing the distribution of degree of steepness of all values in the whole, which reflected the relative sharpness or flatness of a distribution compared with normal distribution.

A positive peak indicated a sharper distribution than normal distribution and a negative peak indicated a flatter distribution than normal distribution. However, no significant difference was found, possibly due to the small sample size of the fact that there were 3 times as many ependymomas as CPPs.

Mean and ADC percentile values

The mean and ADC percentile values of CNCs were significantly lower than those of ependymomas, and the result was similar to those reported previously [13]. Bull et al. found that the mean ADC and the max of ADC of CPPs were significantly higher than those of ependymomas, and the min of ADC of CPPs were slightly lower than those of ependymomas [11]. However, ADC histograms of CPPs and ependymomas were not found to be significantly different in Bonferroni correction in our study. There have been previous studies on differential diagnosis of CPPs and CNCs in MRI [11], but our study used a new method to analyze them. We found that mean, perc.01%, perc.10%, perc.50%, and perc.90% of CPPs were significantly higher than those of the CNCs. Correspondingly, those parameters had relatively good AUC values, with high sensitivity (100%). Kang et al. and Woo et al. reported that low ADC value reflected high cell compositions and high ADC value was correlated with mucoprotein [14,15]. Therefore,

we assumed that the tumor cellularity and mucoprotein component of CPPs were higher than those of CNCs. Further research with larger samples is needed.

Our study had some limitations. The size of the sample was small, the number of patients for each tumor was unbalanced, and further studies with larger sample sizes are needed. In addition, a manually traced boundary has unavoidable errors. Finally, conventional MRI features sometimes fail to differentiate among typical ependymomas, CPPs, and CNCs. Further studies using conventional MRI features, histograms of T2WI, and enhanced-T1WI are warranted.

Conclusions

This study shows that histograms of ADC can improve the diagnostic performance to differentiate among ependymomas, CPPs, and CNCs.

References:

1. Winkler D, Lindner D, Richter A et al: The value of intraoperative smear examination of stereotaxic brain specimens. Minim Invasive Neurosurg, 2006; 49(6): 353–56

2. Yuh EL, Barkovich AJ, Gupta N: Imaging of ependymomas: MRI and CT. Childs Nerv Syst, 2009; 25(10): 1203–13

3. Muly S, Liu S, Lee R et al: MRI of intracranial intraventricular lesions[J]. Clin Imaging, 2018; 52: 226–39

4. Ma Z, Yan H, Shi H et al: The typical and atypical MR imaging findings of central neurocytomas: Report on eighteen cases and review of the literature. Clin Neurol Neurosurg, 2016; 146: 18–23

5. Tien RD: Intraventricular mass lesions of the brain: CT and MR findings. Am J Roentgenol, 1991; 157(6): 1283–90

6. Smoker WR, Townsend JJ, Reichman MV: Neurocytoma accompanied by intraventricular hemorrhage: case report and literature review. Am J Neuroradiol, 1991; 12(4): 765–70

7. Borja MJ, Plaza MJ, Altman N et al: Conventional and advanced MRI features of pediatric intracranial tumors: Supratentorial tumors. Am J Roentgenol, 2013; 200(5): W483–503

8. Tlili-Graiess K, Mama N, Arifa N et al: Diffusion-weighted MR imaging and proton MR spectroscopy findings of central neurocytoma with pathological correlation. J Neuroradiol, 2014; 41(4): 243–50

9. Payabvash S, Tihan T, Cha S: Volumetric voxelwise apparent diffusion coefficient histogram analysis for differentiation of the fourth ventricular tumors. Neuroradiol J, 2018; 31(6): 554–64

10. Rodriguez GD, Awwad A, Meijer L et al: Metrics and textural features of MRI diffusion to improve classification of pediatric posterior fossa tumors. Am J Neuroradiol, 2014; 35(5): 1009–15

11. Bull JG, Saunders DE, Clark CA: Discrimination of paediatric brain tumours using apparent diffusion coefficient histograms. Eur Radiol, 2012; 22(2): 447–57

12. Wang Y J, Xu X Q, Hu H et al: Histogram analysis of apparent diffusion coefficient maps for the differentiation between lymphoma and metastatic lymph nodes of squamous cell carcinoma in head and neck region. Acta Radiol, 2018; 59(6): 672–80

13. Yu Y, Zhang H, Xiao Z et al: Diffusion-weighted MRI combined with susceptibility-weighted MRI: Added diagnostic value for 4 common lateral ventricular tumors. Acta Radiol, 2018; 59(8): 980–87

14. Kang Y, Choi SH, Kim YJ et al: Gliomas: Histogram analysis of apparent diffusion coefficient maps with standard- or high-b-value diffusion-weighted MR imaging – correlation with tumor grade. Radiology, 2011; 261(3): 882–90

15. Woo S, Cho JY, Kim SY et al: Histogram analysis of apparent diffusion coefficient map of diffusion-weighted MRI in endometrial cancer: A preliminary correlation study with histological grade. Acta Radiol, 2014; 55(10): 1270–77